E1-2004-79

INVESTIGATION OF NEUTRON SPECTRA AND TRANSMUTATION OF ^{129}I, ^{237}Np AND OTHER NUCLIDES WITH 1.5 GeV PROTONS FROM THE DUBNA NUCLOTRON USING THE ELECTRONUCLEAR SETUP «ENERGY PLUS TRANSMUTATION»

Submitted to «Nuclear Instruments and Methods in Physics Research A» and presented at the XVII International Baldin Seminar on High Energy Physics Problems «Relativistic Nuclear Physics and Quantum Chromodynamics», September 27 – October 2, 2004, Dubna, Russia

Кривопустов М. И. и др. E1-2004-79
Исследование спектров нейтронов и трансмутации радиоактивных отходов ^{129}I, ^{237}Np и других нуклидов на пучке протонов дубненского нуклотрона с энергией 1,5 ГэВ на установке «Энергия плюс трансмутация»

Описаны эксперименты по программе «Исследование физических аспектов электроядерного способа производства энергии и трансмутации радиоактивных отходов атомной энергетики на пучках синхрофазотрона/нуклотрона ОИЯИ» — проект «Энергия плюс трансмутация». Результаты получены с использованием большой свинцовой мишени с четырехсекционным урановым бланкетом (масса 206,4 кг естественного урана) на пучке нового сверхпроводящего ускорителя — нуклотрона с энергией протонов 1,5 ГэВ. Для регистрации излучений (нейтронов, гамма-квантов и осколков деления) применялись ядерные эмульсии, активационные (^{27}Al, ^{59}Co, ^{127}I, ^{139}La, ^{197}Au, ^{209}Bi) и твердотельные трековые (радиаторы из естественного и обогащенного урана) детекторы. В поле электроядерных нейтронов исследовались трансмутации нуклидов ^{129}I и ^{237}Np (масса каждого изотопа около 1 г) — высокотоксичных долгоживущих радиоактивных отходов атомной энергетики (экологический аспект).

Экспериментальные результаты, полученные из наблюдений (n,xn)-реакций на ядрах Co, Au, Bi и подтвержденные теоретическими расчетами, показывают, что в объеме U/Pb-сборки и на ее поверхности преобладают нейтроны промежуточных и высоких энергий. Из данных (n,γ)-реакции на активационных детекторах из лантана получено, что выход тепловых нейтронов на поверхности уранового бланкета в несколько раз меньше по сравнению со свинцовой мишенью, окруженной парафиновым замедлителем. В настоящей работе впервые в электроядерных экспериментах применена методика ядерных эмульсий для изучения спектров быстрых нейтронов, генерируемых в уран-свинцовой сборке.

Работа выполнена в Лаборатории высоких энергий им. В. И. Векслера и А. М. Балдина ОИЯИ.

Препринт Объединенного института ядерных исследований. Дубна, 2004

Krivopustov M. I. et al. E1-2004-79
Investigation of Neutron Spectra and Transmutation of ^{129}I, ^{237}Np and Other Nuclides with 1.5 GeV Protons from the Dubna Nuclotron Using the Electronuclear Setup «Energy plus Transmutation»

Experiments which are part of the scientific program «Investigations of physical aspects of electronuclear method of energy production and transmutation for radioactive waste of atomic energetics using relativistic beams from the JINR Synchrophasotron/Nuclotron» (project «Energy plus Transmutation») are described. A large lead target surrounded by a four-section uranium blanket with total weight of 206.4 kg natural uranium was irradiated with 1.5 GeV protons from the new cryogenic accelerator Nuclotron. Radiochemical sensors were exposed to the secondary particle fluences inside and on top of the target assembly. Two long-lived radioactive waste of atomic energetics sensors ^{129}I and ^{237}Np (approximately 1 g weight each) and stable nuclides ^{27}Al, ^{59}Co, ^{127}I, ^{139}La, ^{197}Au and ^{209}Bi as well as natural and enriched uranium were used. In addition, various solid state nuclear track detectors and nuclear emulsions were exposed simultaneously. The experimental results confirm the theoretical estimations that the neutron spectra around the U/Pb-assembly are dominated by medium- and high-energy neutrons as shown by the observation of (n,xn)-reaction products in Co, Au and Bi sensors. The yield of thermal neutrons on the surface of the U-blanket is strongly reduced as compared to the surface of a smaller Pb target surrounded with paraffin. The latter data were determined with (n,γ) reactions in stable La sensors. In this experiment the technique of nuclear emulsions has been applied for the first time to measurements of neutron spectra in an accelerator driven system.

The investigation has been performed at the Veksler and Baldin Laboratory of High Energies, JINR.

Preprint of the Joint Institute for Nuclear Research. Dubna, 2004

The authors of the international collaboration started in 1998 for realization of scientific program of the project «Energy plus Transmutation» dedicate this article to cherished memory of Academician of Russian Academy of Sciences **Alexander Mikhailovich Baldin** for his effective support of investigation of electronuclear method of energy production and transmutation of radioactive waste of atomic energetics (ecological aspect) with help of relativistic beams of Synchrophasotron/Nuclotron of JINR's Laboratory of High Energies.

INTRODUCTION

The Veksler–Baldin Laboratory of High Energies within the Joint Institute for Nuclear Research (JINR) in Dubna (Russia) is carrying out extended ***«Investigations of physical aspects of electronuclear method of energy production and transmutation for radioactive waste of atomic energetics using relativistic beams from the JINR Synchrophasotron/Nuclotron» — «Energy plus Transmutation»*** project. It has been introduced into the nuclear science community by Krivopustov et al. [1, 2]. The scientific program (see next page), the experimental setup «Energy plus Transmutation» scheme with lead target and uranium blanket and complex of detectors forming *uranium fission calorimeter* are presented in Fig. 1. It is part of the experimental program at the new cryogenic accelerator Nuclotron, as outlined by Baldin et al. [3]. Basic technical details of this new accelerator have been described by Kovalenko et al. [4]. Results from the first experiment within this series with protons of 1.5 GeV energy impinging onto a lead target that was surrounded by a two-section uranium blanket (with total weight of 103.2 kg natural uranium) have been published [1, 2] and various other papers describe some special aspects of this work [5–11].

The present work describes the experiment with 1.5 GeV protons irradiating a lead target inside a four-section uranium blanket (containing a total of 206.4 kg natural uranium). This continuation of the earlier experiment is dealing with following aspects:

• Transmutation studies on long-lived radioactive waste nuclides ^{129}I and ^{237}Np in the field of secondary neutrons that complement earlier studies (ecological aspect) [13–16].

Program for the experimental studies within the frame of the project «Energy plus Trunsmutation» with lead target and uranium blanket and comlex of detectors forming uranium fission calorimeter [1,2]

P R O G R A M	• Heat generation and energy costs of neutron generation • Neutron multiplication and balance • Energetics gain (power amplification coefficient) • Accumulation of long-lived radioactive products • Transmutation cross-sections of radioactive wastes: α-actinides, fission fragments and activation products • Optimization of parameters of electronuclear installation • Practical recommendations on development of a prototype transmutation installation • Benchmark data to modernize computer codes and programs to simulate electronuclear processes

The uranium fission calorimeter includes the following detector systems on relativistic beams from the JINR Synchrophasotron/Nuclotron:

HPGe – spectrometers	Solid State Nuclear Track Detectors
• Radioactivity of detector monitoring • Distribution of (n, γ)-reaction rate in the blanket • $(n, xnyp)$-reaction distribution in the target • Radioactivity and mass spectrum of nuclides in the activation foils • Distribution of fission fragments in the uranium blanket	• Beam profile and monitoring • Distribution of fissions in the blanket • Integrals of uranium fission induced by thermal, resonance and fast neutrons • Fission density in the lead beam monitor • Average fission cross-section ratio in uranium blanket

Neutron spectrometers (Bonner spheres, activation detectors)	Methods of heat measurements: microthermocouples, quartz resonator, platinum sensors and detectors of infrared radiation
• Specific neutron yields • Neutron energy spectrum • Space distribution of neutrons in the uranium blanket	• Distribution of heat generation over the volume of the uranium blanket and lead converter-target • Specific heat generation in the uranium blanket

• Energy and intensity distributions of neutrons inside and around the U/Pb-assemby studied with $(n,\ \gamma)$ and $(n,\ xn)$ reactions using Al, Co, Au, Bi and La as radiochemical sensors.

• Energy and intensity distributions of neutrons around the target assembly using Solid State Nuclear Track Detectors (SSNTD) and uranium sensors.

• Energy spectra of neutrons using nuclear emulsion techniques (see Ref. [12]).

• Theoretical model calculations of neutron spectra.

The experiment was carried out in 11–12 December 2001 by several groups forming an international team. At first a description of the experimental setup consisting of the lead target, the uranium blanket and the biological shielding will be presented. Second, various experimental studies using different detection systems will be described in detail together with results and theoretical interpretations.

1. EXPERIMENTAL APPARATUS

The lead target together with the four-section uranium blanket is called U/Pb-assembly and is shown in Fig. 1. The lead target has a length of 48 cm and a diameter of 8.4 cm. It is surrounded by four sections of a natural uranium blanket. Each section contains 30 uranium rods. The uranium rods of 10.4 cm length, 3.6 cm diameter and 1.72 kg weight are hermetically sealed in an aluminum cladding. Each section contains 51.6 kg natural uranium and the total uranium content in four sections is 206.4 kg. The construction of the metal structure used to mount the blanket provides a rigid and safe fixation of the uranium rods. The three gaps between the four sections as well as the front and back end of the setup are measuring positions for five large planar detector holder plates (called «Activation and SSNT detectors») as shown in Fig. 1. These detector plates are covered with various SSNTD and activation sensors. In addition to these detectors measuring radial distributions, various sensors were placed on the outside surfaces of each of the four uranium sections. As an example, the position of the placement for the radioactive waste nuclides ^{129}I and ^{237}Np on top of the second section is also indicated in Fig. 1.

The U/Pb-assembly was placed into an external shielding as shown in Fig. 2. The technical design of this shield was made by the Design Institute of Nuclear Power Mashine Building (VNIIAM, Moscow, Russia). This biological shielding is an important safety requirement for such a massive uranium blanket around a lead target that is irradiated with relativistic protons. The big shielding consists of a container filled with granulated polyethylene, and walls are plated with sheets of cadmium and lead. High-energy neutrons are moderated within the polyethylene down to thermal energies. The 1 mm thick Cd-absorbers located at the inner walls of the container reduce significantly the backscattering of thermalized neutrons into the target and detector volume. The outside dimensions of this shielding

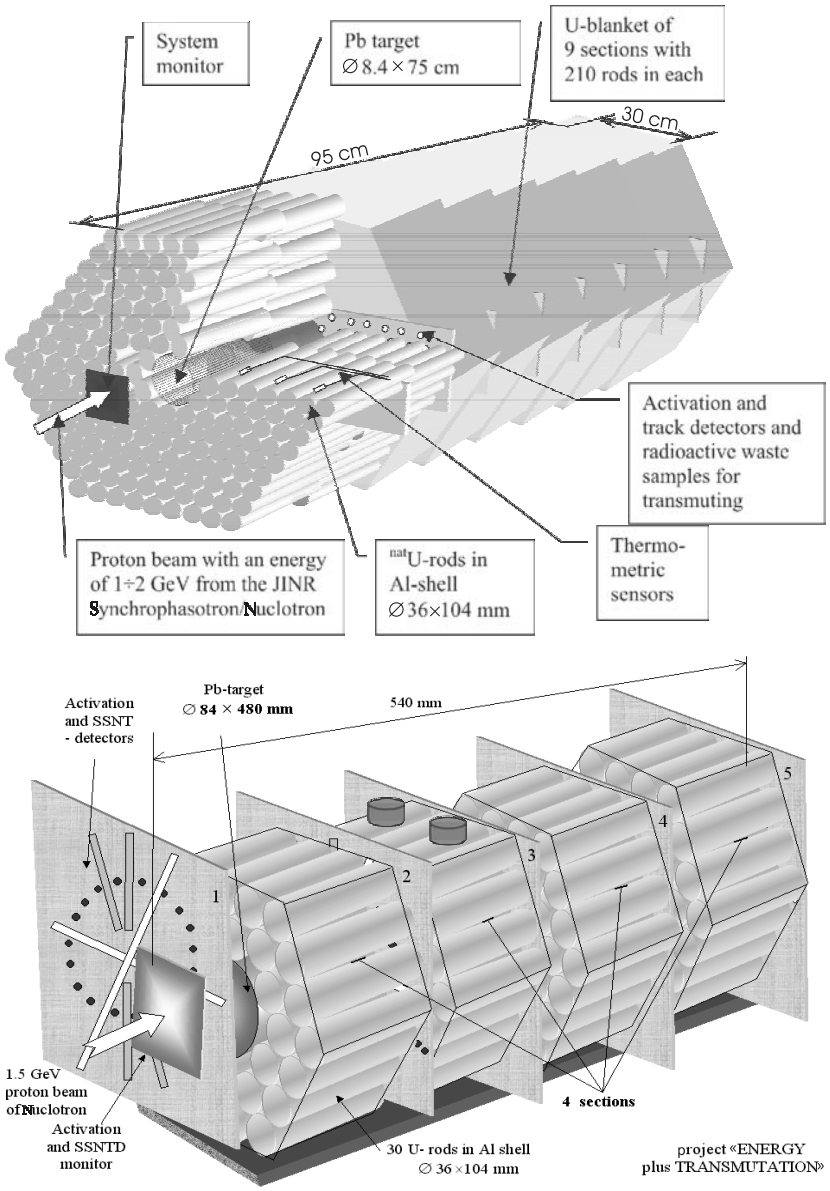

Fig. 1. Scheme of full scale (upper part) and four sections (down part) U/Pb-assembly with uranium blanket around a massive lead target [1, 2]

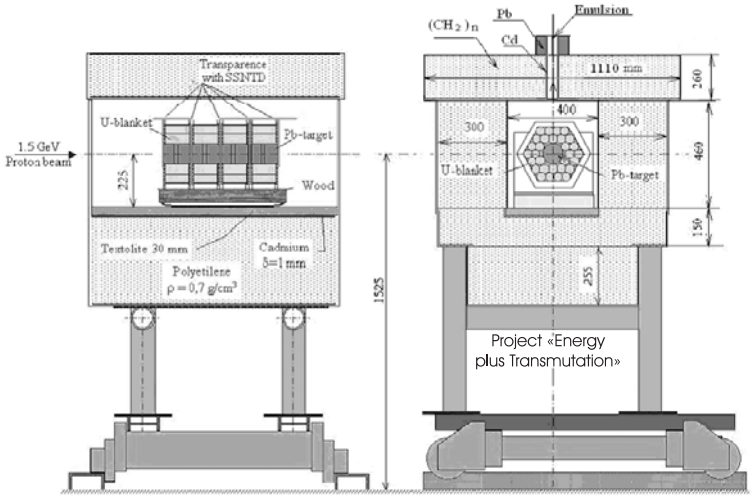

Fig. 2. Technical details of the U/Pb-assembly [1, 2] inside a massive shielding and placed into a mobile platform, which can be moved into and out of the proton beam line. The left side of this figure gives a cut through the assembly along the proton beam line, the right side shows a cut through the assembly perpendicular to the proton beam line in the position where there is a hole within the upside shielding between the 1st and 2nd uranium section

container are $100 \times 106 \times 111$ cm and it has a total weight of 950 kg. It is mounted onto a mobile platform, that can be moved into and later out of the irradiation position called «Focus F3» of the proton exit channel for the Nuclotron beam in the experimental hall. The metallic structure of the biological shielding was manufactured at the Laboratory of High Energies (JINR, Dubna). The left part of Fig. 2 shows a «cut» through the entire assembly along the proton beam line, and the right part of this figure shows the cut through the entire assembly perpendicular to the proton beam line in the position, where there is a hole within the upside shielding. On top of this hole one can directly measure high-energy neutrons emitted from the U/Pb-assembly with nuclear emulsions [12], as described in Sec. 3.3. A more detailed description and technical drawings of details have been published elsewhere [1].

The extracted 1.5 GeV proton beam from the Nuclotron enters the experimental hall with a nominal intensity of $1.5 \cdot 10^{10}$ protons per pulse, the duration of a slow extraction of one pulse lasts 0.3 s, and the repetition rate is one pulse per 9 s. The exact geometrical adjustment of the U/Pb-assembly with respect to the proton beam direction is performed with sensitive Polaroid films and ionization chambers [1, 2]. The accurate monitoring of the proton beam together with the

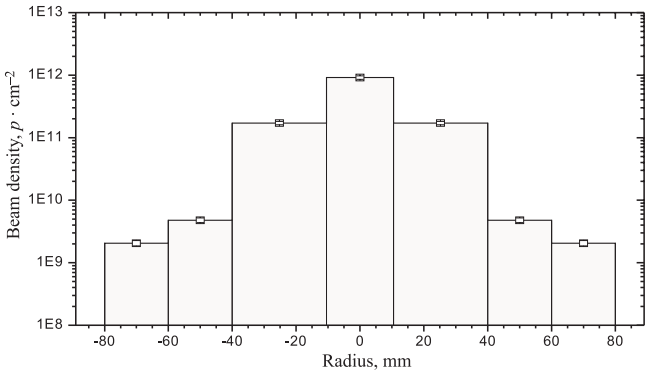

Fig. 3. The beam profile of the 1.5 GeV proton beam from the Nuclotron as it enters the U/Pb-assembly (experiment of 11–12 December 2001)

determination of the integral proton fluence is carried out during the entire run using standard aluminum foil activation detectors. The Al-monitor foils were placed 60 cm upstream the entrance of the protons into the lead target in order to avoid interactions of backscattered neutrons with the monitor foils. Details on the beam monitoring system in the «Focus F3» position have already been published [1, 2]. The monitor reaction ^{27}Al$(p,\ 3pn)^{24}$Na was used to determine the proton fluence where the decay of the ^{24}Na activity was measured using gamma-ray spectrometry [1, 2, 17–20]. The Al-foil of thickness 0.05 mm was cut into 3 concentric rings with external diameters of 80, 120 and 160 mm. From the central part of the Al-foil a circle with diameter of 21 mm was cut out. The cross section used for the ^{27}Al$(p,\ 3pn)^{24}$Na reaction at 1.5 GeV proton energy is (9.93 ± 0.17) mb [20]. The results of beam monitoring are shown in Fig. 3 and in Table 1. The total beam intensity in F3 was $(1.14 \pm 0.06) \cdot 10^{13}$ protons. The central part of the beam with 84 mm diameter, i.e. the diameter of the Pb target (Fig. 1), contained $(1.10 \pm 0.05) \cdot 10^{13}$ protons or $(95.8 \pm 4.7)\,\%$ of the entire beam. This measurement shows that the Nuclotron delivers well-focussed proton beams into the external experimental hall.

Table 1. **Results from the measurement of the beam profile**

External diameter of ring or circle, mm	^{24} Na activity at end of bombardment, Bq	Beam intensity, protons/cm^2
21 (circle)	53.6 ± 3.3	$(9.12 \pm 0.57)\,\mathrm{E}+11$
80	149 ± 9	$(1.72 \pm 0.11)\,\mathrm{E}+11$
120	5.6 ± 0.5	$(4.79 \pm 0.40)\,\mathrm{E}+09$
160	3.3 ± 0.4	$(2.06 \pm 0.21)\,\mathrm{E}+09$

2. EXPERIMENTAL RESULTS BASED ON RADIOCHEMICAL TECHNIQUES

2.1. Spatial Distributions of Neutrons Inside and Around the U/Pb-Assembly Studied with (n,γ) and (n,xn) Reactions Using Al, Co, Au and Bi as Radiochemical Sensors. The spatial and energy distributions of neutrons produced at different locations of the U/Pb-assembly were studied with various radiochemical sensors. Neutrons induce in these activation sensors (metallic foils) radioactive products through (n,xn), (n,α), (n,γ) and other reactions. Different thresholds of these reactions allow one to probe energy spectra of neutrons. Four types of foils (Al, Co, Au and Bi) were placed at different positions within the U/Pb-assembly including also a position inside the lead target. The activation sensors of the first set were placed onto five plates (called «Activation and SSNT detectors» in Figs. 1 and 2) at longitudinal distances of 0, 11.8, 24.0, 36.2 and 48.4 cm from the front of the target and at a radial distance of 3 cm from the target axis. The second set consisted of detectors at a longitudinal distance of 11.8 cm from the front of the target and at radial distances of 3.0; 6.0; 8.5 and 13.5 cm from the target axis. The exact geometrical positions are indicated in Fig. 4.

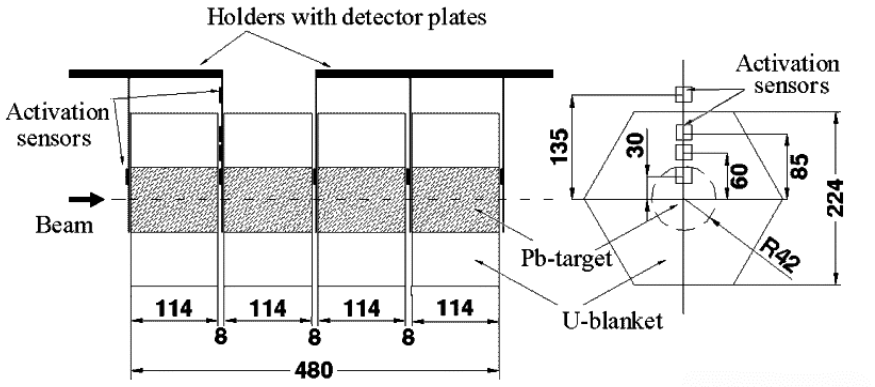

Fig. 4. Positions of various activation sensors within the U/Pb-assembly, including positions inside the Pb target (see Figs. 1 and 2)

After irradiation the activated foils were transported to a counting laboratory in order to investigate the activities with germanium detectors. The characteristics of HPGe detectors and measuring conditions were the same as in other activation experiments described in this paper and they are standard for radiochemical investigations as described in earlier publications [1, 2, 14, 17, 20]. Gamma-ray spectra were analyzed and net peak areas were calculated using the program DEIMOS [21]. Corrections for coincidence summing and background contributions were applied. Thus, decay rates of the produced radioactive nuclides were determined.

Activities at the end of bombardment were converted into production rates $B(A)$ of the produced isotopes A according to the definition [17, 20]:

$$B(A) = (\text{number of } A\text{-atoms produced})/[(1 \text{ g sensor}) \cdot (1 \text{ primary proton})]. \quad (1)$$

$B(A)$ is an absolute number of atoms A produced in the given experimental setup. This production rate is strictly an experimental value which is sensitive to the neutron spectrum at the actual geometric location of the sensor. B values on a given setup are comparable among each other; however, B values measured on different setups are not.

Table 2. **Measured isotopes and features of production and decay**

Foil	Reaction	Produced isotope	$T_{1/2}$, h	$E_{\rm thr}$*, MeV	Gamma-ray lines used, keV
^{197}Au	(n,γ)	^{198}Au	64.68	—	411.8; 675.9; 1087.7
	$(n,2n)$	^{196}Au	148.39	~ 8.1	333.0; 355.7; 426.0
	$(n,4n)$	^{194}Au	38.02	~ 23.2	293.5; 328.5
	$(n,5n)$	^{193}Au	17.65	~ 30.2	173.5; 186.2; 255.6;
	$(n,6n)$	^{192}Au	4.94	~ 38.9	295.9; 308.5; 316.5; 612.5
	$(n,7n)$	^{191}Au	3.18	~ 45.7	277.9; 283.9
^{209}Bi	$(n,4n)$	^{206}Bi	149.83	~ 22.6	343.5; 516.1; 803.0; 881.0
	$(n,5n)$	^{205}Bi	367.44	~ 29.6	703.3; 987.8; 1764.4
	$(n,6n)$	^{204}Bi	11.22	~ 38.1	670.7; 899.2; 918.4; 984.0
	$(n,7n)$	^{203}Bi	11.76	~ 45.2	722.4; 820.2; 825.2
	$(n,8n)$	^{202}Bi	1.72	~ 54.0	422.2; 657.5; 960.7
	$(n,9n)$	^{201}Bi	1.80	~ 61.4	629.1; 936.2; 1014.1
^{59}Co	(n,γ)	^{60}Co	46202.4	-	1173.2; 1332.5
	$(n,2n)$	^{58}Co	1700.64	~ 10.6	810.8
	$(n,3n)$	^{57}Co	6521.76	~ 19.4	122.1; 136.5
	$(n,4n)$	^{56}Co	1853.59	~ 30.9	846.8; 1238.3
	$(n,5n)$	^{55}Co	17.53	~ 41.2	931.3
^{27}Al	$(n,3pn)$	^{24}Na	14.95	~ 5.5**	1368.6; 2754.0

*Nuclear masses for the calculation of $E_{\rm thr}$ were taken from [22].

**Experimental threshold $E_{\rm thr}$ is influenced by the Coulomb barrier.

Each sensor foil was measured twice at different times after irradiation to identify isotopes with different decay times. The results from the analysis of several gamma lines from two spectra were used to calculate the experimental production rate $B(A)$. Weighted averages over the number of spectra were determined for each individual isotope and foil. Resulting values were used for further analysis. Measured isotopes and features of their production reactions and decay are given in Table 2. Results for the longitudinal and radial distributions

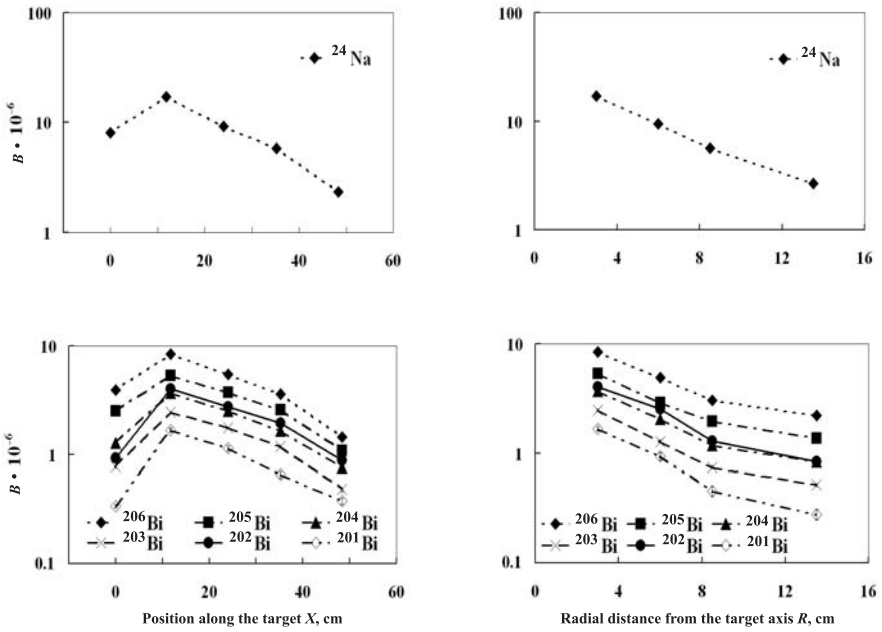

Fig. 5. Production rates $B(A)$ in units of $(10^{-6} \cdot g^{-1} \cdot \text{proton}^{-1})$ for different radioactive isotopes A produced in Al- and Bi-sensor foils. Longitudinal distributions of $B(A)$ are given on the left side and radial distributions on the right side. The lines are drawn to guide eyes

of production rates $B(A)$ for different isotopes are shown in Figs. 5 and 6 where longitudinal distributions are shown on the left side and radial distributions on the right side. Examples of the $B(A)$ values for various geometrical positions are listed in Table 3. The distributions of production rates of $(n,\ xn)$ reactions as a function of the longitudinal distance X from the front of the target have maxima near to the data point at 11.8 cm from the front of the Pb target. The similar trend was observed in case of bare lead target [25].

The production rates of $(n,\ xn)$ reactions monotonically decrease with the radial distance R from the target axis at the longitudinal position $X = 11.8$ cm. Ratios between the production rates at the longitudinal distance X for 0 to 11.8 cm and 11.8 to 48.4 cm (as listed in Table 3) are shown as a function of the reaction threshold energy in Fig. 7.

The resulting experimental trends clearly indicate the increasing contribution of high-energy neutron components with increasing distance X from the front of the target. In contrast to that, the ratio of production rates at radial distances R of 13.5 and 3.0 cm in the direction perpendicular to the target axis at the

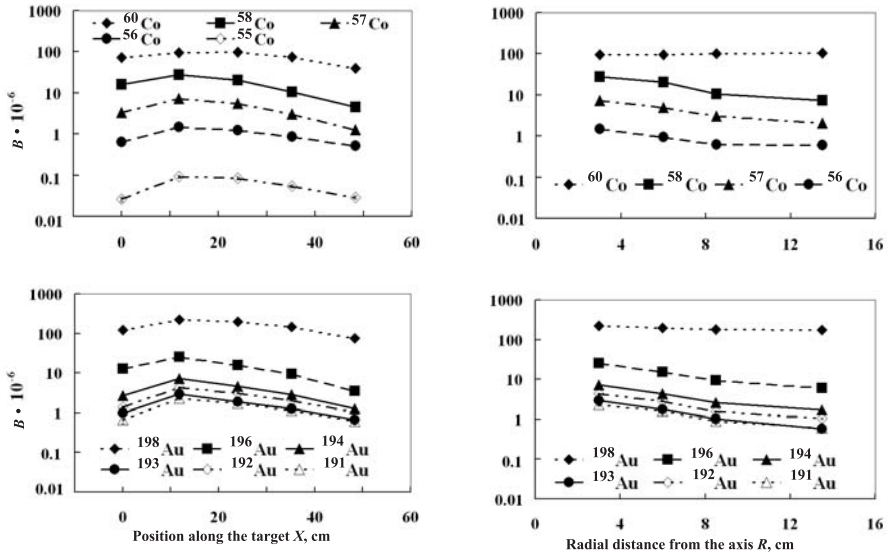

Fig. 6. Production rates $B(A)$ in units of $(10^{-6} \cdot g^{-1} \cdot \text{proton}^{-1})$ for different radioactive isotopes A produced in Co- and Au-sensor foils. Longitudinal distributions of $B(A)$ are given on the left side and radial distributions on the right side. The lines are drawn to guide eyes

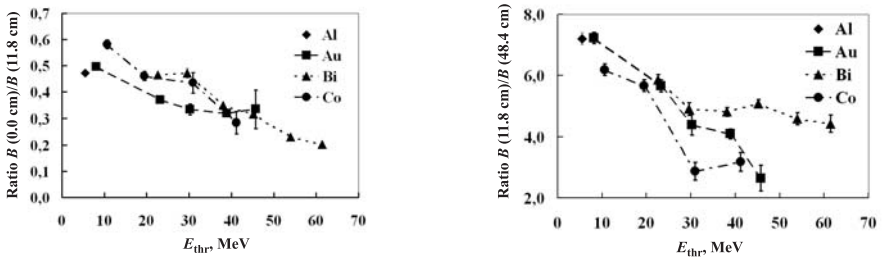

Fig. 7. Ratios of B values inside the Pb target (at a radial distance of $R = 3$ cm) in the front and in the rear of the U/Pb-assembly as a function of the reaction threshold energy

longitudinal position $X = 11.8$ cm are not significantly dependent on threshold energy as shown in Fig. 8. Therefore the shape of neutron's energy distribution does not change much along the radial distance R at the longitudinal distance of 11.8 cm. In contrast with above described behavior of (n, xn) reaction's rates, the distributions of the production rates is more or less flat for (n, γ) nuclear

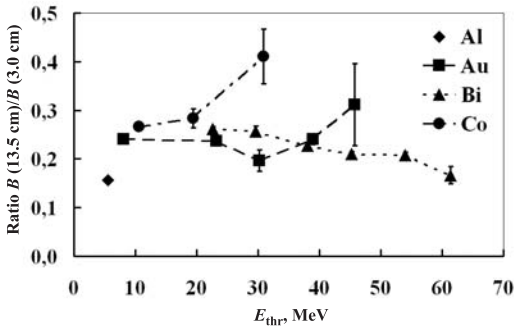

Fig. 8. Ratios between production rates measured in the first gap at radial distances of 13.5 and 3.0 cm from the target axis as a function of the reaction threshold energy $E_{\rm thr}$

Table 3. **Production rates** $B(A) \cdot 10^6$ **for four detector positions**

(X, R), cm*	(0.0, 3.0)	(11.8, 3.0)	(48.4, 3.0)	(11.8, 13.5)
^{24}Na	8.03(20)	17.0(4)	2.36(6)	2.66(7)
^{198}Au	124(3)	220(5)	76.1(2)	177(4)
^{196}Au	12.61(27)	25.4(6)	3.51(9)	6.11(16)
^{194}Au	2.69(8)	7.26(21)	1.28(4)	1.72(6)
^{193}Au	0.99(6)	2.97(14)	0.68(5)	0.59(7)
^{192}Au	1.39(6)	4.36(16)	1.06(4)	1.05(5)
^{191}Au	0.67(14)	1.99(19)	0.75(12)	0.62(17)
^{206}Bi	3.94(5)	8.46(15)	1.44(4)	2.21(4)
^{205}Bi	2.52(10)	5.33(17)	1.09(5)	1.37(6)
^{204}Bi	1.281(19)	3.68(7)	0.763(24)	0.838(20)
^{203}Bi	0.775(18)	2.46(7)	0.484(21)	0.516(18)
^{202}Bi	0.934(16)	4.04(12)	0.88(4)	0.840(27)
^{201}Bi	0.339(13)	1.67(8)	0.377(24)	0.28(3)
^{60}Co	71.8(2)	95(4)	39.6(1)	105(5)
^{58}Co	16.2(5)	27.9(9)	4.50(14)	7.43(26)
^{57}Co	3.35(13)	7.27(26)	1.28(4)	2.06(14)
^{56}Co	0.64(6)	1.47(11)	0.51(5)	0.61(8)
^{55}Co	0.026(4)	0.092(7)	0.0290(28)	—

* X is the longitudinal distance from the beam entrance into the Pb-target, R is the radial distance from the target symmetry axis.

reactions in both longitudinal and radial directions. As these reactions have practically no threshold in neutron energy they probe distributions of «thermal» neutrons. Therefore, the fluency of thermal neutrons seems to be constant over the volume of uranium assembly, see also results obtained with La sensors given below.

To conclude this section, the comparison between experimental and simulated production rates of isotopes, where the energy threshold for production is high makes possible to test the accuracy of the model description of neutron production over a wide interval of neutron energies. It may also be possible to generate the neutron spectrum using the cross-section dependence on neutron energy, provided that a sufficient number of threshold reaction products are available (see Sec. 2.3 and Fig. 11).

2.2. Radiochemical Studies of the Transmutation of Stable ^{139}La. The stable and monoisotopic sensor ^{139}La was used to measure thermal neutron fluences within a small and well-defined volume of approximately 2.5 cm^3 during irradiations with relativistic hadrons onto massive targets, as it was described recently [17, 20, 23]. The same ^{139}La sensors were also used in our studies, using the thermal neutron induced reaction:

$$^{139}\mathrm{La}(n,\gamma)^{140}\mathrm{La}(T_{1/2} = 40.282\ \mathrm{h}) \rightarrow ^{140}\ \mathrm{Ce}\ (\mathrm{stable}). \qquad (2)$$

Ten small plastic vials 15 mm diameter and 50 mm length containing about 1 g La each in the form of $LaCl_3{\cdot}7H_2O$ have been placed along the top surface of the 48 cm long U/Pb-assembly (Figs. 1 and 2) and irradiated with secondary particles. No particular moderator material was inserted between the U/Pb-assembly and the La sensors. The induced ^{140}La activity was measured after the end of irradiation using HPGe-detection systems together with well-known analyzing techniques [18, 19]. The resulting production rate for ^{140}La is given in the form of an experimental $B(^{140}\mathrm{La})$ value, as defined in Eq. (1) above.

Experimental $B(^{140}\mathrm{La})$ values are presented in Table 4 and in Fig. 9 together with equivalent data measured on a Pb/paraffin-assembly [17]. The neutron spectrum in the latter experiment was softened through a 6 cm thick paraffin moderator but there was no shield around the setup. Both data sets were measured with 1.5 GeV proton energy. It is found that the 48 cm long Pb-target with the four-section uranium blanket has an almost constant thermal neutron fluence over nearly its entire length. In contrast, the much shorter 20 cm Pb target with paraffin moderator [17, 20] has a considerably higher and well-accumulated fluence of thermal neutrons. The reason for the missing enhancement of slow neutrons around 15 cm after beam impact into the U/Pb-assembly is qualitatively clear. There is experimental evidence for an enhancement of fast neutrons around 15 cm after beam impact (see Sec. 2.1 and Figs. 5 and 6) but there is no suitable moderating material available to slow these fast neutrons down. The inner side of the external shield is covered with a Cd layer, thus preventing thermalized neutrons from moving back from the shielding or from the environment into the target area. Therefore one expects to find only those thermal neutrons on top of the U/Pb-assembly that were actually produced in the thermal energy regime or that were thermalized through collisions with atoms in the target and blanket or

Table 4. $B(^{140}\mathbf{La})$ **values at 1.5 GeV proton energy using different target systems**

Longitudinal distance X from beam entrance to sensor in mm	$B(^{140}\mathrm{La}) \cdot 10^5$ fast neutron spectrum (this work)	$B(^{140}\mathrm{La}) \cdot 10^5$ moderated neutron spectrum (Ref. 17)
20	1.18 ± 0.06	—
53	—	5.45 ± 0.43
55	1.33 ± 0.07	—
95	1.49 ± 0.08	—
101	—	8.40 ± 0.64
149	—	8.10 ± 0.64
199	—	5.71 ± 0.45
210	1.48 ± 0.08	—
249	—	3.25 ± 0.26
265	1.46 ± 0.08	—
300	1.48 ± 0.08	—
345	1.31 ± 0.07	—
385	1.11 ± 0.06	—
425	0.96 ± 0.05	—
465	0.80 ± 0.08	—

that migrated back from the shield without being caught by the Cd layer. As the energy loss in a collision between a neutron and heavy atoms like Pb or U is small one needs many collisions to slow down neutrons to thermal energies. As a consequence, the initially focussed direction of motion of the neutrons is lost and the measured distribution is flat.

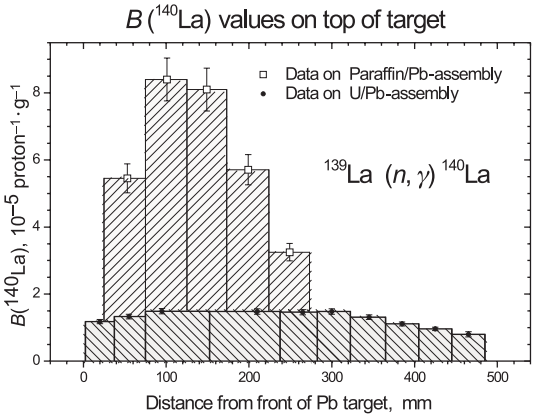

Fig. 9. The dependence of the measured $B(^{140}\mathrm{La})$ yields along the proton beam direction on top of the target in two experiments: U/Pb-assembly (this experiment) and Pb target with paraffin moderator [17]

2.3. Transmutation of Radioactive Waste Nuclides ^{129}I and ^{237}Np and stable ^{127}I. The transmutation of long-lived radioactive waste into stable or short-lived radioactive nuclides is of major interest in these studies. Transmutation cross sections (B values) are ideal benchmark data to test theoretical models that describe the complex process of interactions of the primary beam, the production of spallation neutrons, secondary reactions in the assembly, particle transport properties and finally the interaction with the sensor nuclide. The correct description of all processes is an essential premise for credible results from the necessary calculations that must be made in order to design a real transmutation setup on the technical or even industrial scale. The nuclides ^{129}I and ^{237}Np are of particular practical interest, as they are long-lived radioactive waste nuclides from nuclear facilities and they can be transmuted with neutrons into stable or short-lived isotopes:

$$^{129}\mathrm{I}(T_{1/2} = 1.57 \cdot 10^7 \text{ y})(n,\gamma) \rightarrow^{130} \mathrm{I}(T_{1/2} = 12.4 \text{ h}) \rightarrow^{130} \mathrm{Xe\ (stable)}, \quad (3)$$

$$^{237}\mathrm{Np}(T_{1/2} = 2.14 \cdot 10^6 \text{ y})(n,\gamma) \rightarrow^{238} \mathrm{Np}(2.12 \text{ d}) \rightarrow^{238} \mathrm{Pu}(T_{1/2} = 88 \text{ y}). \quad (4)$$

As available ^{129}I sensors from radioactive waste reprocessing are a mixture of 15% stable ^{127}I and 85% radioactive ^{129}I, it appeared to be useful to study simultaneously the transmutation of pure ^{127}I samples. The available ^{237}Np sensor is isotopically pure. Sample containers used are shown schematically in Fig. 10. The $^{127,\ 129}$I in the form of NaI salt is hermetically sealed in a welded aluminum container and the sensor has been manufactured at the Institute of Physics and Power Engineering (Obninsk, Russia). The radioactive sample contained 0.772 g ^{129}I plus 0.136 g ^{127}I. Two inactive iodine control sensors contained 1.439 g ^{127}I each. The radioactive ^{237}Np sample contained 1.061 g ^{237}Np in the chemical form NpO_2. All sensors were placed on top of the second uranium section, as counted downstream from the beam entrance into the lead target and irradiated during the entire experiment. Afterwards, all sensors were investigated with standard gamma-ray spectroscopy as described earlier. Because of the high level of radioactivity induced in the massive Al container (78.8 g Al) the gamma detector was shielded with 2 mm Cd and 2 mm Cu filters in order to reduce the background. Further details of the gamma-spectrum analyzing procedures for this special case are given in [24]. Changes in the beam intensity during the irradiation were taken into account for the calculation of the experimental $B(A)_{\mathrm{exp}}$ values for the various radioactive transmutation products. Results are given in Table 5 together with theoretical estimations for $B(A)_{\mathrm{cal}}$ values, based on a modified LAHET-code [25] as described below.

The calculation of $B(^{128-121}\mathrm{I})_{\mathrm{exp}}$ for a pure ^{127}I sensor is carried out by taking the results of measured B_{exp} values for the mixture of the (^{129}I plus ^{127}I) sensor and for a pure ^{127}I sensor, using straightforward arithmetic.

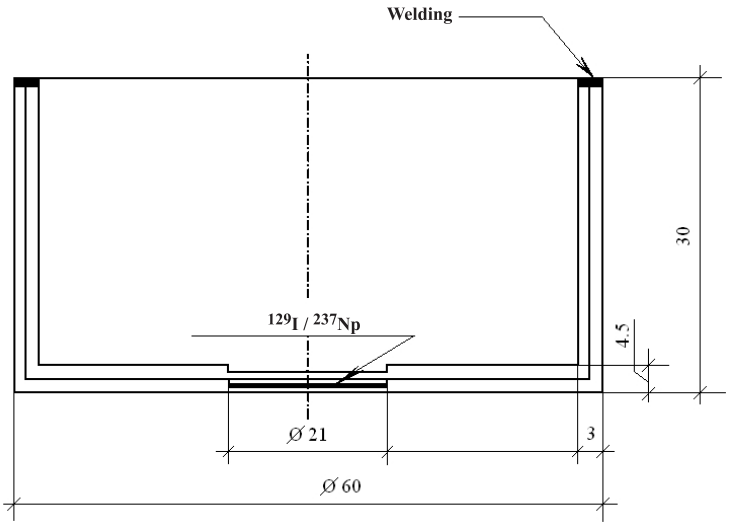

Fig. 10. Weld-sealed aluminum containers used for radioactive sensors like ^{129}I or ^{237}Np and used for transmutation experiments (see Ref. [13])

Table 5. **Experimental and calculated $B(A)$ values in Np, I, Al sensors at 1.5 GeV proton energy**

Isotope	$T_{1/2}$, h, d, min	$B(A)_{\rm exp} \cdot 10^6$ in ^{237}Np, ^{129}I and ^{27}Al sensors	$B(A)_{\rm cal} \cdot 10^6$ in ^{129}I or ^{27}Al sensors, LAHET calculation	$B(A)_{\rm exp} \cdot 10^6$ in ^{129}I or ^{27}Al sensors	$B(A)_{\rm cal} \cdot 10^6$ in ^{129}I or ^{27}Al sensors, LAHET calculation
^{238}Np	2.12 d	24.6 ± 1.3	—	—	—
^{130}I	12.3 h	32.5 ± 1.7	—	—	—
^{128}I	25 min	—	—	93 ± 7	—
^{126}I	13.1 d	1.28 ± 0.11	0.48	5.0 ± 0.5	0.42
^{124}I	4.17 d	0.362 ± 0.030	0.124	1.40 ± 0.10	0.07
^{123}I	13.3 h	—	—	0.82 ± 0.10	0.05
^{121}I	2.12 h	—	—	0.28 ± 0.07	0.07
^{120}I	81 min	—	—	0.084 ± 0.015	0.03
^{24}Na	14.95 h	2.00 ± 0.16*	1.21	5.14 ± 0.30	1,96

* This value agrees fairly well with an independent determination given in Table 3 for $X = 11.8$ cm and $R = 13.5$ cm.

In other experiments the transmutation of ^{129}I was investigated using a massive setup and higher proton energy. Due to the different beam energy and geometric differences of setups the results of the measurements of this and the other experiment are incomparable. Details are given in [23, 25].

In contrast to other transmutation studies [13, 14, 20, 23] with thermalized neutrons, one observes in this experiment some $(n,\ \gamma)$ reactions as well as substantial contributions from $(n,\ xn)$ reactions, leading to very neutron deficient iodine isotopes such as ^{120}I. A model-based calculation was carried out for reaction rates $R_{\rm cal}$ according to the equation

$$R_{\rm cal} = \int_{E_{\rm thr}}^{E_{\rm max}} \sigma(E_n)\Phi(E_n)dE_n, \tag{5}$$

where $E_{\rm thr}$ is the threshold energy for a particular reaction channel. The value $\Phi(E_n)$ is the neutron fluence $[n \cdot {\rm cm}^{-2} \cdot {\rm MeV}^{-1} \cdot p^{-1}]$ and it is calculated using the program DCM/CEM [26, 27] for the given geometry of the experiment (see below). The calculated reaction rate $R_{\rm cal}$ is related to the calculated $B_{\rm cal}$ value as follows:

$$R_{\rm cal}(^{130-121}{\rm I}) = B_{\rm cal}(^{130-121}{\rm I}) \cdot A/N_A, \tag{6}$$

where A is the mass number and N_A is Avogadro's number. Cross sections for $^{129}{\rm I}(n,\ xn)$ and $^{127}{\rm I}(n,\ xn)$ reactions are calculated by means of a modified program LAHET [25] depending on the neutron energy. Calculated values $B_{\rm cal}$ and experimental data $B_{\rm exp}$ from Table 5 show that the agreement of these values is far from being satisfactory due to the inaccuracy of calculations of either neutron cross sections and/or the energy-dependent neutron fluence.

In order to estimate the neutron spectrum from our experimental data, an approach was suggested starting with experimental reaction rates $R_{\rm exp}$ (or $B_{\rm exp}$ values) from Table 5 and calculated values of cross sections of $(n,\ xn)$ reactions as a function of neutron energy [25].

Let $R_i({\rm exp})$ and $\sigma_i(E_n)$ correspond respectively to the reaction rate of the reaction with emission of i neutrons and to the calculated cross section of this reaction for the neutron energy E_n. Reactions with removal of a maximum of 8 neutrons are observed in our experiment starting with ^{127}I. Thus

$$R_8({\rm exp}) = \int_{E^{(8)}_{\rm thr}}^{E_{\rm max}} \varphi_8(E_n)\sigma_8(E_n)dE_n \approx \overline{\varphi_8(E_n)} \int_{E^{(8)}_{\rm thr}}^{E_{\rm max}} \sigma_8(E_n)dE_n. \tag{7}$$

Therefore $\overline{\varphi_8(E_n)}$ was calculated, which is the average value of the neutron fluence in the energy range from $E^{(8)}_{\rm thr} = 68$ MeV up to $E_{\rm max} = 300$ MeV. In case of a reaction with emission of 7 neutrons the following relation applies:

$$R_7({\rm exp}) = \overline{\varphi_7(E_n)} \int_{E^{(7)}_{\rm thr}}^{E^{8}_{\rm thr}} \sigma_7(E_n)dE_n + \overline{\varphi_8(E_n)} \int_{E^{(8)}_{\rm thr}}^{E_{\rm max}} \sigma_7(E_n)dE_n, \tag{8}$$

which allows one to determine $\overline{\varphi_7(E_n)}$. Experimental values of $R_5({\rm exp})$, $R_4({\rm exp})$ and $R_2({\rm exp})$ were used in a similar manner to determine average neutron fluences

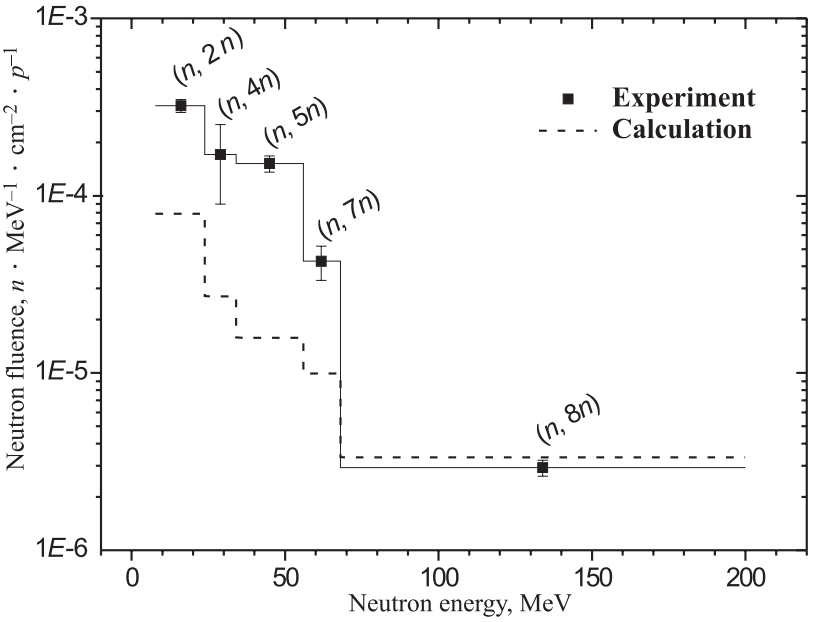

Fig. 11. Experimental neutron spectrum at 1.5 GeV extracted from product yields of $(n,\ xn)$ reactions in ^{127}I on top of the U/Pb-assembly and comparison with the calculated neutron spectrum based on the DCM/CEM-code [26, 27]

$\overline{\varphi_5(E_n)}$, $\overline{\varphi_4(E_n)}$ and $\overline{\varphi_2(E_n)}$ in the energy ranges $(E_{\mathrm{thr}}^{(5)},\ E_{\mathrm{thr}}^{(7)})$, $(E_{\mathrm{thr}}^{(4)},\ E_{\mathrm{thr}}^{(5)})$ and $(E_{\mathrm{thr}}^{(2)},\ E_{\mathrm{thr}}^{(4)})$, respectively.

The resulting experimental neutron spectrum and the appropriately averaged calculated neutron spectrum are shown in Fig. 11. The agreement between these two spectra is not at all satisfactory.

2.4. Further Computer Simulations on Neutron Induced Transmutation of ^{127}I and ^{129}I. The spectra of secondary particles (neutrons and protons) crossing the external surface of the U/Pb-assembly were calculated with the assumption of an ideal non-absorbing detector by means of the program DCM/CEM [26, 27]. The range of neutron energies extends from thermal up to 300 MeV. It is assumed in the calculations that the temperature of the lead target and the uranium blanket is thermal (0.0252 eV).

In principle, one can register particles with larger energies up to the initial bombarding energy of 1.5 GeV. However, due to an insignificant amount of such particles, they were not considered in calculations. The energy range of secondary protons is considered within the limits from the cut-off energy ($\sim$ 2 MeV) up to 300 MeV. Calculations of energy spectra of secondary particles were performed as before [1, 2, 7, 26, 27].

The energy range of secondary particles below 10.5 MeV is divided up according to the 26 group system. Additional splitting of the energy range < 0.1 eV is introduced to describe the thermalized spectrum. The energy range > 10.5 MeV is divided with a step width of 10 MeV. Additional calculations of the neutron spectra above the threshold of several nuclear reactions ^{129}I $(n,\ 4n)^{126}$I and ^{127}I $(n,\ 2n)^{126}$I were carried out with smaller step (2 MeV) to study the features of these reactions under conditions of irradiation of the samples of ^{127}I and ^{129}I.

Neutron spectra are registered in geometrical positions corresponding to the actual locations of radioactive ^{129}I, ^{127}I and ^{237}Np sensors in this experiment. Geometrical features and chemical composition of the lead target, natural uranium blanket and radiation shielding and moderator containing sheets of cadmium, lead and granulated polyethylene (see Fig. 2) are considered in very detail in calculations. However, we had to make the assumption that the medium in the limits of separate geometrical zones is homogeneous (in the case of the blanket this assumption is a crude approximation because in the real assembly this volume is filled with cylindrical uranium rods). Therefore we introduced a correction to the density of the volume taking into account the porosity of the medium. Furthermore, an assumption was also made concerning the shape of the blanket. The hexagonal sections (see Figs. 1 and 2) were replaced in the calculations with an equivalent cylinder. There was no acceptable agreement between the calculated neutron spectra and other experimental data.

The cross sections of $(n,\ xn)$ reactions on ^{127}I and ^{129}I using the same programs were also calculated (see Table 5). The calculation was performed by modeling of inelastic interactions of neutrons with subsequent normalization of the fraction of the given reaction channel on the calculated inelastic cross section. Reactions for the production of isotope ^{126}I from ^{129}I and ^{127}I nuclei are characterized by a pronounced peak in the energy distribution of the cross section which is in the region of 30 MeV for the reaction ^{129}I$(n,\ 4n)^{126}$I and of around 20 MeV for the reaction ^{127}I$(n,\ 2n)^{126}$I, respectively.

The data of this section were compared with the data received by means of the modified program LAHET [25]. It is found that the results calculated with the program LAHET appear to be systematically lower by a factor of 2.5 in the region of the maximum in comparison to the data received with the program DCM/CEM [1, 2, 26, 27]. The overall agreement between experimental and calculated results, however, is poor.

It is necessary to note the contribution of the proton component to the amount of induced activities. Cross sections of threshold reactions ^{129}I$(p,\ p3n)^{126}$I and ^{127}I$(p,\ pn)^{126}$I differ from corresponding neutron reactions by a shift in the reaction threshold to higher energies. The shift is in value approximately equal to the binding energy of the nucleon in the nucleus. The contribution of the proton component to the total ^{126}I activity is about two orders of magnitude below the corresponding contribution of the neutron fluence.

3. EXPERIMENTS USING SOLID STATE NUCLEAR TRACK DETECTORS

3.1. Space and Energy Distribution of Neutrons Determined with Mica Detectors. The determination of the spatial and energy distribution of neutrons in the U/Pb-assembly (Fig. 1) using solid state nuclear track detectors included the measurement of distributions of ^{235}U and ^{238}U fission rates and the determination of the spectral index: $\bar{\sigma}_f^{^{238}\mathrm{U}}/\bar{\sigma}_f^{^{235}\mathrm{U}}$, where $\bar{\sigma}_f^{^{235}\mathrm{U}}$ and $\bar{\sigma}_f^{^{238}\mathrm{U}}$ are the fission cross sections, respectively, for ^{235}U and ^{238}U averaged over the neutron spectrum.

Spectral indices are based on observed fission rates within the Pb target and U blanket as described in detail in [8]. The aim of measurements of ^{235}U and ^{238}U fission rates and spectral indices is to obtain information about the neutron field in the system, integral nuclear data and the determination of the total number of fission events within the uranium blanket. A comparison of the experimental data with the calculated results was carried out using Monte Carlo simulations with the adjusted computer code DCM/CEM [28] and a library of hadron-nuclear cross sections [29]. Libraries for neutron cross sections were applied [30, 31] when calculating the fission rates and spectral indices.

Measurements were carried out with SSNTD as described earlier [8]. The sensors consisting of fissionable sources and track detectors for fission fragments were placed onto detector plates, labelled «Activation and SSNT detectors» (Fig. 1). On each of the five detector plates in the U/Pb-assembly six sensor positions were used, radially distributed from the lead target axis to the outer surface of the U blanket. The two innermost positions were situated inside of the lead target, three positions within the uranium blanket, and one position outside of the blanket. All five detector plates were identically constructed.

Metallic foils from 90% enriched ^{235}U and from natural uranium of 7 mm diameter and approximately 0.1 mm thick were used as fissioning sources. They were manufactured by cold rolling and vacuum annealing of the material. The advantage of using thick sources is the fact that there is no necessity for thickness calibration of each individual source and that the sensitivity is optimized. Artificial mica (fluoroflogopite) was used as the fission fragment detector. A compilation of all results from the experiment will be given in a forthcoming publication [32].

In Fig. 12 we present the results of measurements and calculations of the radial distribution of ^{235}U and ^{238}U fission rates as measured in the second detector plate, which is at 11.8 cm from the front of the lead target. Fission rates of both nuclides ^{235}U and ^{238}U decrease inside the blanket with increasing radial distance R from the axis of the U/Pb-assembly by factors of approximately 1.3 for ^{235}U and, depending on the detector plate, between 2.6 and 3.5 for ^{238}U, as compared to a calculated decrease by factors of 1.6 and between 2.2 and 3.8, respectively. It is seen, that the value of decrease of the fission rate for ^{238}U is much larger than for the ^{235}U fission rate. It can be explained by the

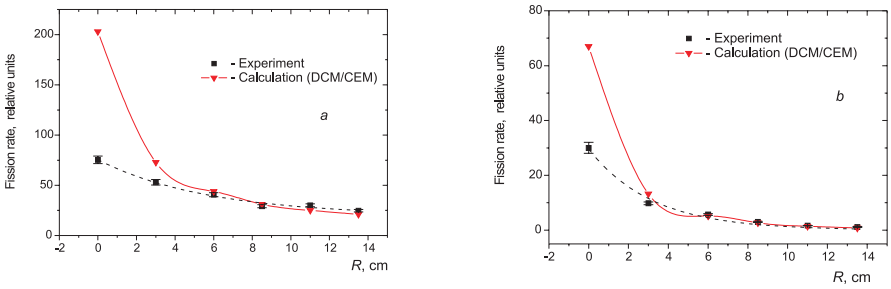

Fig. 12. Radial distributions of fission rates for ^{235}U (*a*) and ^{238}U (*b*) inside the Pb target and U blanket (see Fig. 1) measured in the second detector plate. The Pb target extends up to $R = 4.2$ cm and the U blanket up to $R = 13.5$ cm. R is the radial distance from the axis of the lead target. The lines are drawn to guide the eyes

fact that the decrease of neutron fluence density in radial direction connected with an absorption in the blanket material and the effect of geometric factor is compensated by an increase of the average cross section of ^{235}U fission caused by a decrease in the average energy of neutrons.

For a somewhat qualitative understanding of measured fission rates the central data point at $R = 0$ cm, i.e. measured at the axis of the lead target, shall be omitted. Fission rates at this point will be caused by interactions from neutrons and other secondary hadrons as well as from the primary protons of the beam, at least in the first plates. For larger values of R the direct influence of the primary proton beam can be neglected. To a first approximation the neutron density will be «diluted» with rising distance R from the beam axis, where the dilution scales somewhere between $1/R$ and $1/R^2$. The dilution function is not well defined because neutrons are produced in an extended volume and by several production modes. Assuming the extreme dilution function $1/R^2$ which applies for a point source only, one yields «dilution factors» of 4, 8, 13 and 20 when R increases from 3.0 to 6.0; 8.5; 11.0 and 13.5 cm, respectively. Experimentally measured fission rates for ^{238}U scale, in fact, approximately with these dilution factors, however, they are higher than these by a factor of about 2 for all distances R greater than 3 cm, i.e. outside of the Pb target and inside the U blanket. Thus, the density of neutrons having an energy above the fission threshold for ^{238}U of about 1.4 MeV is constantly an «excess factor» of 2 higher than that produced by spallation reactions in the lead target and measured at $R = 3$ cm.

For fission rates of ^{235}U we find a completely different dependence. The experimental fission rates do not decrease in parallel with the dilution factors, but there is rather a significant increase of the excess factor, which in turn scales linearly with rising R. The excess of low-energy neutrons that induce fission of ^{235}U is a factor of 3.1 higher than expected at $R = 6$ cm and it is 9.3 times higher

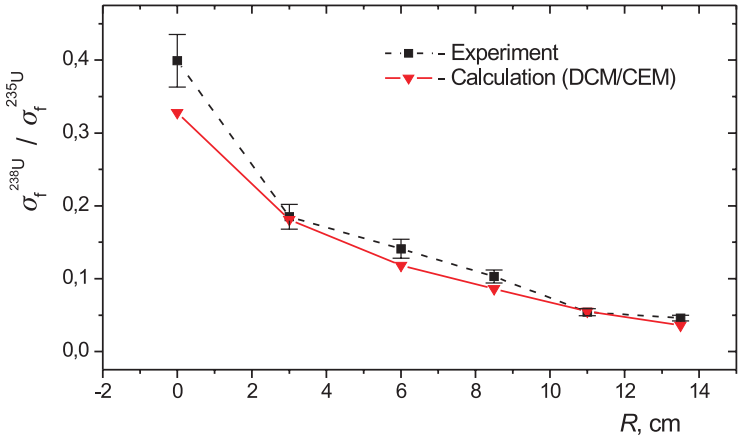

Fig. 13. Radial distribution of spectral index $\bar{\sigma}_f^{238\mathrm{U}}/\bar{\sigma}_f^{235\mathrm{U}}$ within the Pb target and the U blanket for the second plate (see Fig. 1). The lines are drawn to guide the eyes

at $R = 13.5$ cm. These excess low-energy neutrons must be generated through secondary reactions as well as by moderation of spallation neutrons originating from the primary interaction in the lead target.

The results of measurements and calculation of the spectral index $\bar{\sigma}_f^{238\mathrm{U}}/\bar{\sigma}_f^{235\mathrm{U}}$ in dependence of the radial distance R within the U/Pb-assembly for the second detector plate are given in Fig. 13. The good agreement between measurement and calculation of the radial distributions in the ratio of ^{235}U and ^{238}U fission rates shows that the model calculation describes consistently the particles energy transfer within the blanket. The spectral index, which is an indicator of the neutron spectrum hardness, decreases with increasing distance R from the target axis, thus showing the softening of the neutron spectrum in the radial direction.

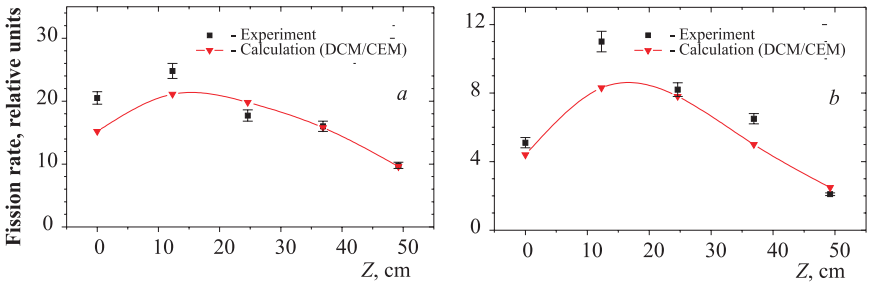

Fig. 14. Longitudinal distributions of fission rates for ^{235}U (*a*) and ^{238}U (*b*) fission rates along the top surface of the U blanket. The lines are drawn to guide the eyes

The experimental and calculated axial distributions of ^{235}U and ^{238}U fission rates exhibit similar features on all five detector plates along the entire target

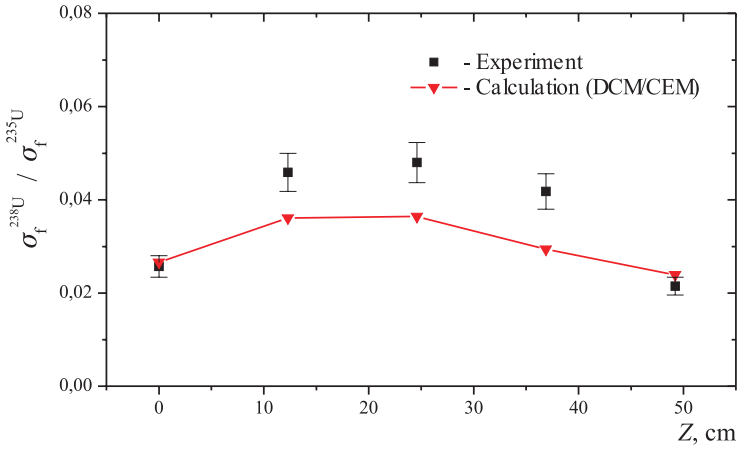

Fig. 15. Longitudinal distribution of spectral index $\bar{\sigma}_f^{238}\mathrm{U}/\bar{\sigma}_f^{235}\mathrm{U}$ along the top surface of the U blanket (see Figs. 1, 2). The line is drawn to guide the eyes

assembly with a maximum of the fission rates in the second detector plate. In Fig. 14 the fission rates of ^{238}U and ^{235}U are shown for all detector plates at a radial distance $R = 13.5$ cm. These positions are on top of the blanket and close to the locations where the radiochemical transmutation sensors were mounted on the surface of the blanket.

Experimental values of the longitudinal distribution of the spectral index do not change significantly along the surface of the U blanket (see Fig. 15) with only some deficiency of fast neutrons around the front and the rear ends of the U/Pb-assembly. The experimental values of the spectral indices are higher than calculated ones by up to 42%, thus indicating that the experimental neutron spectrum is significantly harder than calculated.

3.2. Measurement of Neutron Fluence and Neutron Energy Regimes Using SSNTD. Neutron fluence measurements were performed in the gaps between the U-blanket sections, on surface of the blanket as well as on top of the target shielding using various forms of solid state nuclear track detectors, as indicated in Fig. 16. In each gap between the U-blanket sections, twelve sets of SSNT detectors were placed along the diagonal of the hexagon (along the strip in Fig. 16). On the surface of each section of the U blanket four sets of the detectors were parallel to the beam axis. In addition, at three different positions on the top of the shielding, five sets of SSNT detectors were placed parallel to the beam axis, in order to measure the neutrons escaping from the setup.

Each set of SSNTD provided three different detection areas and it consisted of a CR-39 foil on polyethylene, half-covered with $^{6}Li_2B_4O_7$ convertor material. The area with this convertor was partially covered on both sides with 1 mm of Cd. Such detection system can simultaneously detect thermal and intermediate-fast

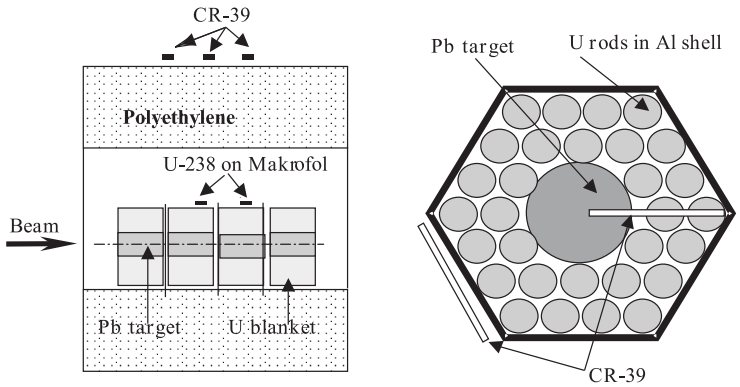

Fig. 16. Positions of SSNT detectors in and on the U/Pb-assembly (see Figs. 1, 2 and 4)

neutrons. The difference in track density between the Cd-covered and uncovered part of the CR-39 foil plus $^{6}Li_2B_4O_7$ converter comes from thermal neutrons which induce (n,α) processes in $^{10}B(n,\alpha)^{7}Li$ and $^{6}Li(n,\alpha)^{3}H$ reactions. The track density in the completely uncovered CR-39 foil (no convertor, no Cd) originates from recoil protons from (n,p) scattering reactions giving indirect information about intermediate energy and fast neutrons in the energy range of $0.3 < E_n < 3$ MeV, which is the range with an about constant response of CR-39 to protons [33]. Details on the operation of these systems and their response are given in [34]. Moreover, SSNTD acting as fission detectors for fast neutrons detection above ~ 1.4 MeV were placed on the top of the middle sections of the U blanket (see Fig. 16). These detectors consisted of Makrofol foils with about 1 mg $\cdot$ cm^{-2} of ^{238}U evaporated on one surface. Details of this method to detect neutrons with energies above ~ 1.4 MeV are given in [35]. After the irradiation with a total of approximately 10^{11} protons the SSNTD etching and track-scanning under an optical microscope was carried out.

Neutron fluence distributions in units of $n \cdot \mathrm{cm}^{-2} \cdot p^{-1}$ measured between the sections of the U blanket are presented in Fig. 17, as a function of the radial distance R from the Pb-target simmetry axis. These neutron distributions are attributed to fast neutrons alone. Thermal neutrons were not detected because their contribution is lower than the detection limit of the detector ($< 10^5\ n \cdot \mathrm{cm}^{-2}$). In all three gaps the neutron density is the highest at the target axis and it drops off towards the surface of the U blanket. The decrease of neutron density in the second and third gap scales approximately with $1/R^2$, where R is the radial distance from the beam axis. The neutron distribution in the fourth gap looks quite different, possibly because protons come to rest after about 30 cm inside the target. Thus, there are no spallation neutrons produced in the central region of the target around the fourth gap and the detected neutrons are only those emitted in forward directions. The different origin of neutrons in the fourth gap is also

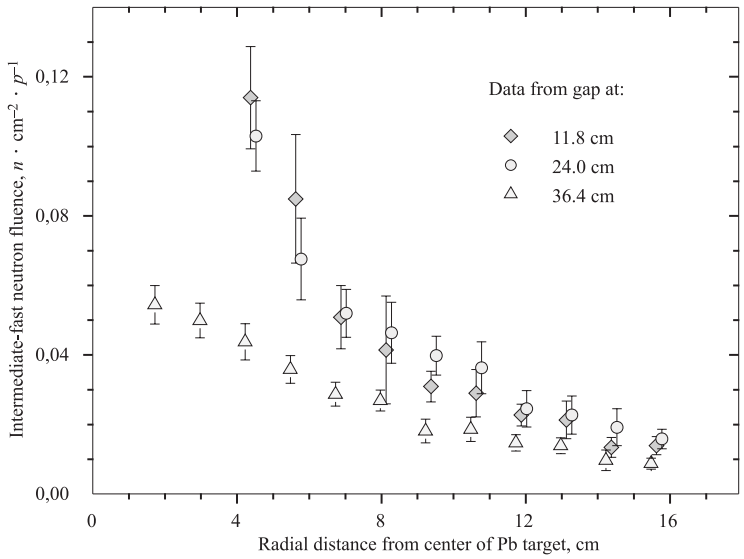

Fig. 17. Intermediate-fast neutron distributions between sections of the U blanket as a function of the radial distance R from the axis of simmetry of the Pb target. The data set from the third gap (at 36.4 cm) is shifted 0.15 cm to the left, the data set from the second gap (at 24.0 cm) is shifted 0.15 cm to the right

evident from the results of a fitting process to the neutron fluence distributions in the radial direction R. The neutron fluence distribution in the fourth gap is described well by the exponential form $Y = A \cdot \mathrm{e}^{BR}$, in contrast to the second and third gap where a power law $Y = A \cdot R^B$ fits best, as shown in Table 6.

Table 6. **Fitting parameters describing the radial decrease of the neutron fluence (see Fig. 17)**

Distance along the target, cm	Fitting model	Parameter A	Parameter B
12.0	$Y = A \cdot R^B$	1.26 ± 0.19	-1.61 ± 0.09
24.2	$Y = A \cdot R^B$	0.71 ± 0.08	-1.33 ± 0.07
36.4	$Y = A \cdot e^{BR}$	0.073 ± 0.002	-0.13 ± 0.01

The four sets of SSNT detectors placed on the surface of each U blanket section showed essentially identical results among each other. So, results presented in Fig. 18 represent the mean value of the four measurements, where the longitudinal distance is measured from the beam entry into the target. Both, thermal and indermediate-fast neutrons were detected in the four positions. The

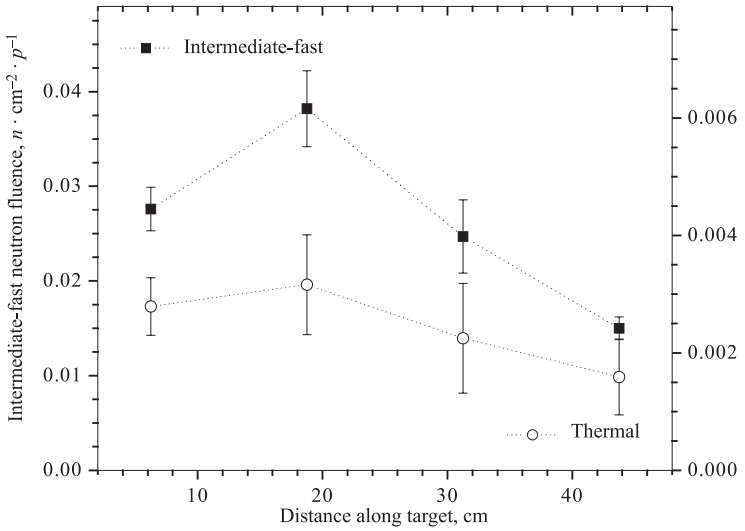

Fig. 18. Thermal and intermediate-fast neutron densities on the surfaces of the four U blanket sections (see Figs. 1, 2 and 16)

intermediate-fast neutron distribution peaks slightly on the second section and then drops significantly towards the end of the target. In contrast to that, the thermal neutrons distribution is essentially flat with only minor deficiencies on the fourth section. The thermal neutron distribution resembles the shape of the radiochemically determined $B(^{140}\mathrm{La})$-value distribution shown in Fig. 9. Densities of thermal neutrons on top of the blanket are one order of magnitude less than indermediate-fast neutrons (see Fig. 18).

The neutron fluence measured with fission detectors on the surface of the second and third sections of the U blanket is presented in Table 7. For comparison, measurements by proton recoils with CR-39 at the same positions are also tabulated. There is a reasonable agreement between the two methods considering the different energy ranges covered by each method.

Table 7. **Fluence of fast neutrons on the surface of the middle sections of the U blanket measured with two different SSNTD methods**

Neutron energy range, eV	Neutron fluence, $10^{-3}\ n \cdot \mathrm{cm}^{-2} \cdot p^{-1}$	
	Proton recoil detectors	Fission fragment detectors
$3 \cdot 10^5$ to $3 \cdot 10^6$	2.5 ± 0.9	—
Above $1 \cdot 10^6$	—	7.5 ± 1.7

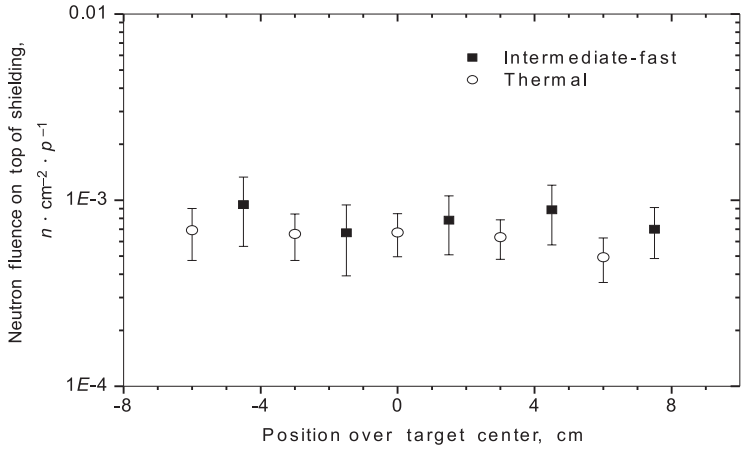

Fig. 19. Experimental thermal and intermediate-fast neutron fluences measured in the middle of the U/Pb-assembly on top of the shielding

The fluence of thermal and intermediate-fast neutrons escaping the polyethylene shielding was measured at three different positions on the top of the shielding, using five sets of CR-39 detectors that were placed vertical to the Pb-target axis (see Fig. 16). The fluences measured at each of the three positions show no significant variations among each other, therefore only the results obtained at the central position are presented in Fig. 19. The total neutron density is about one order of magnitude lower than directly on the U blanket surface and half of the neutrons are in the thermal energy range. Taking into account that 1 mm of Cd on the target side of the shielding box has absorbed all thermal neutrons coming out of the U/Pb-assembly the thermal neutrons on top of the shielding must be decelerated intermediate-fast neutrons. Thus, the polyethylene shielding proves to be an efficient moderator in which half of fast neutrons leaving the U blanket are thermalized. However, neutrons with energies ranging up to 3 MeV were also detected on top of the shielding and therefore in forthcoming experiments the contribution of high-energy neutrons around the whole setup should be measured using U/Makrofol and Au/Makrofol fission detectors.

3.3. Measurements of Fast Neutron Spectra with Nuclear Emulsions. The preceding sections gave a detailed account on neutron spectra measured inside and around the U/Pb-assembly with major emphasis on neutrons with energies below several MeV. An accurate measurement of the neutron spectrum, in particular, of the high energy part above 1 MeV neutron energy, was carried out using nuclear emulsions. Details of this technique have been described in our article (see [12]). The measurement was performed on the outside of the biological shielding above the uranium blanket between the first and second uranium section, such as

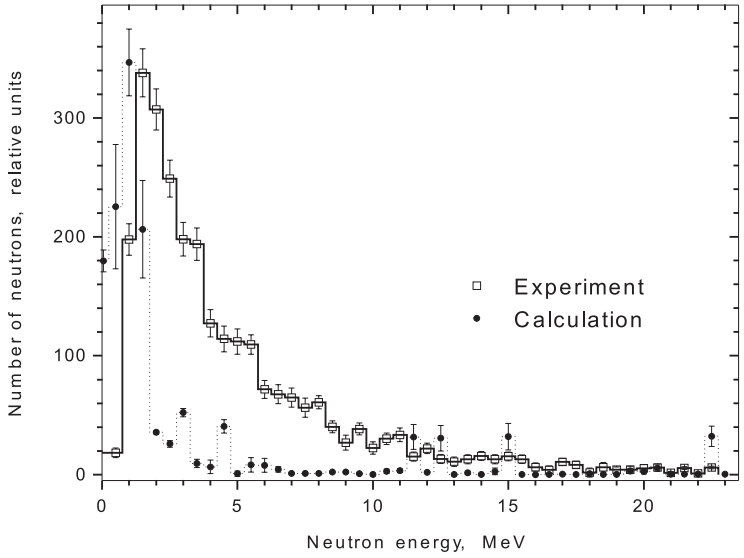

Fig. 20. Experimental and calculated neutron spectrum above the U/Pb-assembly during the irradiation with 1.5 GeV protons

indicated in Fig. 2. The figure shows a cut through the entire U/Pb-assembly and also the hole in the top part of the shielding.

Cd foils aligned around and over this hole prevented the transfer of thermal neutrons through this opening. High sensitivity thick nuclear emulsions G-5 BR (baseless, relativistic) were exposed to neutrons emitted from the uranium blanket that were moving in the 90° direction to beam axis during an irradiation with a few pulses of 1.5 GeV protons. The nuclear emulsion sheet had the size $100 \cdot 25 \cdot 1.4$ mm^3 and it was positioned in 500 mm distance above the top surface of the U blanket. The hole of 30 mm diameter in the top shielding was used as a collimator for the neutrons (see Fig. 2). High-energy neutrons produce recoil protons inside the nuclear emulsion which in turn produce tracks for analysis. After the irradiation proton tracks inside the nuclear emulsion were developed and about 3000 events were scanned and measured with an optical microscope. The accurate measurement of the recoil proton track length allows a very precise determination of the proton energy E_p. The direction of motion of each proton is measured and the scattering angle Θ relative to the direction of the collimating hole is calculated. Thus, it is possible to determine the primary neutron energy E_n of the elastically scattered neutron using the equation $E_n = E_p(\cos\,\Theta)^{-2}$.

The resulting neutron spectrum is shown in Fig. 20 where the maximum of the registered distribution is at (1.5 ± 0.5) MeV neutron energy. Neutron energies up to 200 MeV have been observed. The barycenter of the spectrum from 0 to 20 MeV is at (4.3 ± 0.5) MeV. If statistics could be improved through extensive

scanning of additional tracks one would surely have also registered neutrons of higher energies and the barycenter of the distribution would be slightly over 4.3 MeV. Thus the barycenter of the same spectrum in range from 0 to 50 MeV is at (6.6 ± 0.5) MeV. This neutron spectrum measured over the uranium blanket is much harder than the fission neutron spectrum in a conventional nuclear reactor where the barycenter is (1.58 ± 0.12) MeV (see Fig. 1 and Table 1 in [38]).

The neutron spectrum on top of the shielding is determined experimentally with very good resolution and high statistical significance. This spectrum is therefore very suitable to serve as a benchmark set of data for comparison with model calculations. The theoretical spectrum as calculated with the program DCM/CEM [26, 27] is also indicated in Fig. 20. Significant discrepancies found, especially in the low- and medium-energy region, clearly show that the modelling of neutron production and transport processes needs improvement. As the modelling of the interaction environment was very elaborate in the calculations it may seem that the basic modelling of the physics of interactions has to be improved. Discrepancies found in the emulsion method confirm results from radiochemical measurements with threshold detectors (see Sec. 2.3 and Fig. 11) where similar discrepancies between experimental and calculated neutron spectra were encountered.

CONCLUSIONS

An extended U/Pb-assembly [1, 2] containing a massive 43 kg Pb target surrounded by 206.4 kg natural uranium as U blanket without any low-Z moderators was irradiated with 1.5 GeV protons. Quantitative details of the neutron induced transmutation of nuclides as well as neutron yields and neutron spectra have been investigated within this assembly.

• Due to very hard neutron spectra, one could observe products in stable Co, Au and Bi sensors from $(n,\ xn)$ reactions yielding neutron deficient isotopes produced through the emission of up to $x = 9$ neutrons. This is in contrast to the transmutation yields restricted essentially to (n, γ) processes as observed in an accelerator driven model system containing an efficienct low-Z moderator that produced a high thermal neutron fluence [13, 14, 20, 23].

• For the same reasons, one observed in transmutation studies on the stable nuclide ^{127}I not only the direct (n, γ)-transmutation product ^{128}I but also considerable yields of neutron deficient iodine isotopes down to ^{120}I. Transmutation yields in both systems with hard or soft neutron spectra depend in detail on the actual geometrical construction of the setups.

• Experimental radial and axial distributions of ^{235}U and ^{238}U fission rates, as well as spectral indexes $\bar{\sigma}_f^{^{238}\mathrm{U}}/\bar{\sigma}_f^{^{235}\mathrm{U}}$ have been obtained with the SSNTD method for the entire Pb target and the U blanket. Calculated results using a modified computer code DCM/CEM show a reasonable agreement with the experimental

radial and axial distributions of ^{235}U and ^{238}U fission rates inside the blanket and a less satisfactory agreement on the surface of the blanket. Experimental and calculated results for spectral indexes $\bar{\sigma}_f^{^{238}\mathrm{U}}/\bar{\sigma}_f^{^{235}\mathrm{U}}$ do not change within the range of experimental uncertainties on the surface of the blanket in the axial direction. This indicates a rather constant neutron spectrum in the U/Pb-assembly along the proton beam direction. The agreement of the measured and calculated results confirms the fact that the calculation model describes correctly the relative energy transfer due to scattering within the blanket material.

• Results of ^{235}U and ^{238}U fission rates are confirmed by a second set of SSNTD experiments using CR-39 and Macrofol plastic track detectors, where the fast neutron fluence on the U-blanket surface is studied over its total length. Taking the measured neutron fluences on the surface of the U blanket as shown in Fig. 18, one can estimate the expected fluence for a 1 mA proton beam of 1.5 GeV in the present system as follows:

$$\Phi \text{ (thermal-epithermal neutrons)} = 1 \cdot 10^{13} \text{ neutrons} \cdot \text{cm}^{-2} \cdot \text{s}^{-1},$$

$$\Phi \text{ (intermediate-fast neutrons)} = 2 \cdot 10^{14} \text{ neutrons} \cdot \text{cm}^{-2} \cdot \text{s}^{-1}.$$

Such neutron fluences are a quite substancial achievement towards the realization of a transmutation facility on a larger scale. However, they request the technical ability to remove considerably more than 1.5 MW of thermal energy out of the assembly which is a difficult technical task.

• The neutron spectrum up to 25 MeV energy was measured with high resolution and good statistical precision using a nuclear emulsion method. The comparison of experimental and calculated data unambiguously shows that current model descriptions for neutron production and transport need improvement. In this experiment the technique of nuclear emulsions has for the first time been applied to measurements of neutron spectra in an accelerator driven system (ADS).

• It is evident from all comparisons shown between experimental data and the results from model calculations that the theoretical modeling of neutron production and transmutation processes needs a lot of improvement. Differences between measured and calculated data by a factor of 20 or more are frequently encountered. Such differences are unacceptable when large transmutation facilities shall designed on a technical or even on an industrial scale.

It is shown, that the project «Energy plus Transmutation» [1, 2] provides valuable results and useful technical informations [5–12] towards the realization of scientifically and industrially relevant future constructions employing accelerator-driven systems.

Acknowledgements. Authors are grateful to Profs. A. I. Malakhov, N. A. Rusakovich and V. B. Brudanin, Drs. Yu. S. Anisimov and P. I. Zarubin for their help with the construction of the installation, preparation and carrying out of the experiments and gamma-spectroscopic measurements. We thank the technical personnel

of the Laboratory of High Energies under the leadership of Prof. A. D. Kovalenko for providing reliable operation of the Nuclotron. Authors are grateful to the Workshop of the Laboratory of High Energies headed by Yu. I. Tyatyushkin for mechanical construction work. Authors express their gratitude to E. M. Pavliouk for assistance in preparing this manuscript.

The enthusiastic scientific and experimental help over many years of Dr. E.-J. Langrock (Hoyerswerda, Germany) is gratefully acknowledged.

Authors are grateful to the Ministry of Atomic Energy of the Russian Federation for providing the material to build the uranium blanket, the main part of the experimental installation «Energy plus Transmutation». Results described in the present work were obtained with the financial support of the FZJ (Jülich, Germany), Russian Foundation for Basic Research (Moscow, Russia) and of the JINR Directorate who provided the operation of the accelerator and reactor installations.

One of the authors (M. I. K.) is grateful to Prof. W. Ensinger (Kernchemie Institut, Fachbereich Chemie Philipps-Universitaet, Marburg, Germany) for creating favorable conditions on the last stage of this work.

REFERENCES

1. *Krivopustov M. I. et al.* On a First Experiment on the Calorimetry of the Uranium Blanket Using the Model of the U/Pb Electro-Nuclear Assembly «Energy plus Transmutation» on a 1.5 GeV Proton Beam of the Dubna Synchrophasotron. JINR Preprint P1-2000-168. Dubna, 2000; Kerntechnik. 2003. V. 68. P. 48–55.

2. *Krivopustov M. I., Chultem D.* Experiments on Electronuclear Technology and Radioactive Waste of Atomic Energetics Transmutation on Beams of the Synchrophasotron JINR Dubna // JINR News. 1998, No. 3;
   Krivopustov M. I. et al. On the First Experiment on Calorimetry of Uranium Blanket of the Model U/Pb-Assembly of the Electronuclear Installation «Energy plus Transmutation» in the 1.5 GeV Proton Beam from the JINR Synchrophasotron // Proc. of the Intern. Seminar on High Energy Physics Problem. Relativistic Nuclear Physics and Quantum Chromodynamic. Dubna, September 25–29, 2000. Dubna, 2001. V. 2. P. 3–21.

3. *Baldin A. M., Malakhov A. I., Sissakian A. N.* Some Problems of Relativistic Nuclear Physics and Multiple Particle Production. JINR Communication P1-2001-106. Dubna, 2001. P. 58–59.

4. *Kovalenko A. D. et al.* The Nuclotron — New Superconducting Ion Synchrotron at JINR // Proc. of the COSPAR Colloquium, Dubna, 2003 (in press); Nuclotron: Main Results and Development Plans // Journ. Atom. Energy. 2002. V. 93. P. 479–485.

5. *Chultem D. et al.* Studies of Fission Fragment Mass Spectra and Yields of $(n,\ \gamma)$- and $(n,\ 2n)$-Reactions in the Subcritical Uranium Blanket of the Installation «Energy

plus Transmutation» at the Proton Beam from the JINR Synchrophasotron at 1.5 GeV. JINR Preprint P1-2002-16. Dubna, 2002.

6. *Krivopustov M. I. et al.* Modelling of the Electronuclear Method of Energy Production and Study of Radioactive Waste Transmutation Using a Proton Beam of the JINR Synchrophasotron/Nuclotron — Project «Energy plus Transmutation». JINR, 99-266. Dubna, 1999. P. 135–139.

7. *Martsynkevich B. A. et al.* Unfolding Neutron Spectra in Wide Energy Range up to 200 MeV in Subcritical Uranium Blanket of the Installation «Energy plus Transmutation». JINR Communication P1-2002-165. Dubna, 2002; // Vesti NASB. Physics-Mathematics Series. Minsk, 2004. V. 1. P. 90–95.

8. *Zhuk I. V. et al.* Investigation of Energy-Space Distribution of Neutrons in the Lead Target and Uranium Blanket within the Installation «Energy plus Transmutation» Exposed to 1.5 GeV Protons. JINR Preprint P1-2002-184. Dubna, 2002; // Vesti NASB. Physics-Technicks Series. Minsk, 2003. V. 12. P. 31–35.

9. *Chultem D., Tumendelger Ts., Krivopustov M. I.* Uranium Fission Track Integrator to Study Heat Generation in the Subcritical Uranium Blanket of Electronuclear Installation. JINR Communication P1-2001-128. Dubna, 2001.

10. *Goncharova L. A. et al.* Automatization of Measurement and Analysis of Track Information on Heat Generation in the Uranium Blanket of Electronuclear System. Preprint 25, RAS Lebedev Institute of Physics. Moscow, 2001.

11. *Brandt R. et al.* Investigation of Temperature and Neutron Fields in Lead Accompanying Interactions of Relativistic Protons. JINR Communication P1-99-117. Dubna, 1999.

12. *Chultem D. et al.* Investigation of Fast Neutron Spectra of the Installation «Energy plus Transmutation» at the 1.5 GeV Proton Beam of the Nuclotron. JINR Preprint P1-2003-59. Dubna, 2003.

13. *Krivopustov M. I. et al.* First Experiments on Transmutation Studies of Iodine-129 and Neptunium-237 Using Relativistic Protons of 3.7 GeV. JINR Prepint E1-97-59. Dubna, 1997; J. of Radioanal. and Nucl. Chem. 1997. V. 222. P. 267.

14. *Wan J. S. et al.* Transmutation of Radioactive Waste with the Help of Relativistic Heavy Ions // Kerntechnik. 1998. V. 63. P. 167.

15. *Adam J. et al.* Investigation of the Formation of Residual Nuclei from the Radioactive ^{237}Np and ^{241}Am Targets in the Reaction with 660 MeV Protons // Nucl. Phys. 2002. V. 65. P. 797.

16. *Adam J. et al.* Investigation of Residual Nuclei in Reactions Induced by 660 MeV Protons Interacting with ^{237}Np, ^{241}Am and ^{129}I Targets // Journ. Nucl. Sci. and Technol. 2002. Suppl. 2. P. 272.

17. *Adam J. et al.* First Nuclear Activation Experiments Using the New Accelerator Nuclotron in Dubna // Kerntechnik. 2003. V. 68. P. 214.

18. *Westmeier W.* Handbuch des Gamma-Spektrenanalyse Programms GAMMAW (10.32). Gesellschaft für Kernspektrometrie. D-35085 Ebsdorfergrund, Germany.

19. *Reus U., Westmeier W.* // At. Data and Nucl. Tables. 1983. V. 29. P. 1.

20. *Westmeier W. et al.* Transmutation Experiments on ^{129}I, ^{139}La and ^{237}Np Using the Nuclotron Accelerator (submitted to Radiochemica Acta).

21. *Frana J.* Program DEIMOS 32 for Gamma-Ray Spectra Evaluation // Radioanal. and Nucl. Chem. 2003. V. 257. P. 583.

22. *Audi G. et al.* The NUBASE Evaluation of Nuclear and Decay Properties // Nucl. Phys. A. 1997. V. 624. P. 1.

23. *Adam J. et al.* Transmutation of ^{239}Pu and Other Nuclides Using Spallation Neutrons Produced by Relativistic Protons Reacting with Massive U- and Pb-Targets // Radiochemica Acta. 2002. V. 90. P. 431.

24. *Adam J. et al.* Program Complex and Ammendments to the Method of Activation Analysis to Determine Cross Sections of Nuclear Reactions // Izmeritelnaya Tekhnika. 2001. P. 57.

25. *Ganusheva D.* Modeling of Neutron Fields for Transmutation of Fission Fragments and Actinides. Dipl. Thesis (Karlow University, Prague, Czech Republic), 2001.

26. *Polanski A., Sosnin A. N., Toneev V. D.* On Anomalous Na-24 Production in High Energy Nuclear Interactions. JINR Preprint E2-91-562. Dubna, 1991.

27. *Sosnin A. N. et al.* Monte Carlo Modelling of Neutron Spectra in the U/Pb-Assembly Irradiated with Protons // Izvestiya RAS. Phys. Ser. 2002. V. 66. P. 1494.

28. *Barashenkov V. S. et al.* Software «Kaskad» for Monte-Carlo Simulation of Nuclear and Physical Processes Initiated by High-Energy Particles and Nuclei in Gaseous and Condensed Media. JINR Preprint P2-85-173. Dubna, 1985.

29. *Barashenkov V. S., Gudowski W., Polanski A.* Integral High-Energy Nucleon-Nucleus Cross-Sections for Mathematical Experiments with Electronuclear Facilities // Proc. of the 3rd Intern. Conf. on Accelerator Driven Transmutation Technologies and Applications — 99'ADTTA, Praha, 7–11 June 1999. MO-O-C10 (CD ROM Edition).

30. *Abagyan L. P. et al.* Group Constants for Calculation of Reactors and Shielding. Reference book. M.: Energoizdat. 1981. P. 231.

31. *Lisowski P. W. et al.* Neutron Induced Fission Cross Section Ratios for ^{232}Th, $^{235,\ 238}$U, ^{237}Np and ^{239}Pu from 1 to 400 MeV // Proc. of the Intern. Conf. on Nuclear Data for Science and Technology. 30 May–3 June 1988, JAERI, Mito, Japan. Mito, 1988.

32. *Zhuk I. V.* Private communication.

33. *Harvey J. R. et al.* The Contribution of Eurados and CENDOS to Etched Track Neutron Dosimetry // Journ. Radiation Protection and Dosimetry. 1998. V. 77. P. 267.

34. *Zamani M., Sampsonidis D., Savvidis E.* An Individual Dosimeter with $(n,\ \gamma)$- and $(n,\ p)$-Converters // Journ. Rad. Meas. 1996. V. 26. P. 87.

35. *Remy D. et al.* // Journ. de Physique. 1970. V. 31. P. 27.

36. *Adloff J. C. et al.* Secondary Neutron Production from Thick Pb Target by Light Particle Irradiation // Journ. Rad. Meas. 1999. V. 31. P. 551.

37. *Wan J. S. et al.* Transmutation of ^{129}I and ^{237}Np Using Spallation Neutrons Produced by 1.5, 3.7 and 7.4 GeV Protons // Journ. Nucl. Instr. Meth. A. 2001. V. 463. P. 634.

38. *Steward L.* Leakage Neutron Spectrum from a Bara ^{239}Pu Critical Assembly // Journ. Nucl. Sci. and Eng. 1960. V. 8. P. 595.

Received on June 23, 2004.

Корректор *Т. Е. Попеко*

Подписано в печать 22.09.2004.
Формат 60 × 90/16. Бумага офсетная. Печать офсетная.
Усл. печ. л. 2,43. Уч.-изд. л. 3,43. Тираж 450 экз. Заказ № 54610.

Издательский отдел Объединенного института ядерных исследований
141980, г. Дубна, Московская обл., ул. Жолио-Кюри, 6.
E-mail: publish@pds.jinr.ru
www.jinr.ru/publish/